



Delft University of Technology

A comprehensive study on the influence of Sasobit content on rheological properties and storage stability of CR/SBS composite-modified asphalt

Zhao, Kangzhi; Li, Yang; He, Fuqiong; Meng, Yuanyuan; Hu, Chichun; Ye, Xiangqian; Lin, Peng

DOI

[10.1016/j.conbuildmat.2025.140066](https://doi.org/10.1016/j.conbuildmat.2025.140066)

Publication date

2025

Document Version

Final published version

Published in

Construction and Building Materials

Citation (APA)

Zhao, K., Li, Y., He, F., Meng, Y., Hu, C., Ye, X., & Lin, P. (2025). A comprehensive study on the influence of Sasobit content on rheological properties and storage stability of CR/SBS composite-modified asphalt. *Construction and Building Materials*, 463, Article 140066. <https://doi.org/10.1016/j.conbuildmat.2025.140066>

Important note

To cite this publication, please use the final published version (if applicable).

Please check the document version above.

Copyright

Other than for strictly personal use, it is not permitted to download, forward or distribute the text or part of it, without the consent of the author(s) and/or copyright holder(s), unless the work is under an open content license such as Creative Commons.

Takedown policy

Please contact us and provide details if you believe this document breaches copyrights.

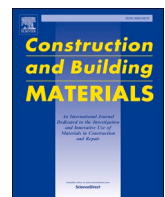
We will remove access to the work immediately and investigate your claim.

Green Open Access added to TU Delft Institutional Repository

'You share, we take care!' - Taverne project

<https://www.openaccess.nl/en/you-share-we-take-care>

Otherwise as indicated in the copyright section: the publisher is the copyright holder of this work and the author uses the Dutch legislation to make this work public.



A comprehensive study on the influence of Sasobit content on rheological properties and storage stability of CR/SBS composite-modified asphalt

Kangzhi Zhao^a, Yang Li^a, Fuqiong He^f, Yuanyuan Meng^d, Chichun Hu^{a,b,*}, Xiangqian Ye^{a,e}, Peng Lin^c

^a College of Civil Engineering & Transportation, South China University of Technology, Guangzhou, Guangdong 510640, China

^b China-Singapore International Joint Research Institute, Guangzhou, Guangdong 510700, China

^c Section of Pavement Engineering, Department of Engineering Structures, Faculty of Civil Engineering and Geosciences, Delft University of Technology, Netherlands

^d School of Intelligent Transportation and Engineering, Guangzhou Maritime University, Guangzhou 510725, China

^e Department of Civil and Architectural Engineering, KTH – Royal Institute of Technology, Stockholm 10044, Sweden

^f Guangdong Dr. Road Traffic Technology Co., Ltd., Guangzhou, Guangdong 510630, China

ARTICLE INFO

Keywords:

CR/SBS composite-modified asphalt

Rheological properties

Sasobit

Storage stability

Workability

ABSTRACT

The CR/SBS composite-modified asphalt (CR/SBS-CMA) is recognized for its excellent rutting and fatigue resistance, but with poor workability. Sasobit has been introduced as an additive to improve the workability of CR/SBS-CMA. This study aims to investigate the effects of Sasobit content on the storage stability and rheological properties of CR/SBS-CMA. The Brookfield viscosity tests were used to measure the viscosity of samples. The Fourier transform infrared spectroscopy (FTIR) tests were conducted to study the modification mechanism. The cigar tube and fluorescence microscopy (FM) tests were employed to study the storage stability of samples. The penetration, softening point, and ductility of samples were assessed. The rheological behaviors of samples were assessed through dynamic shear rheometer (DSR) tests and bending beam rheometer (BBR) tests. The test results indicate that Sasobit can effectively reduce the viscosity of CR/SBS-CMA. Sasobit can also improve the rutting resistance, fatigue resistance, and storage stability of CR/SBS-CMA. However, Sasobit negatively affects the low-temperature performance of CR/SBS-CMA, so its content should be lower than 3 % when applied in areas with low temperatures. This study will contribute to the reduction of energy consumption and greenhouse gas emissions during the construction of CR/SBS-CMA pavement.

1. Introduction

Adding modifiers to virgin asphalt to produce modified asphalt is a mainstream method for enhancing asphalt performance [1]. Hot mix technology is commonly used to apply these modified asphalts for paving [2]. However, this process consumes a significant amount of energy and generates large quantities of greenhouse gases [3]. For high-viscosity modified asphalts, which require higher temperatures to achieve proper compatibility, have more significant construction energy consumption and greenhouse gas emissions [4]. This severely limits the practical use of such modified asphalts in construction. CR/SBS composite-modified asphalt (CR/SBS-CMA), a composite-modified asphalt prepared by incorporating styrene-butadiene-styrene (SBS) and crumb rubber (CR) into virgin asphalt, is a high-viscosity modified asphalt that faces the aforementioned issues [5].

As one of the components of CR/SBS-CMA, SBS is a triblock copolymer made from styrene and butadiene monomers [6]. It is currently one of the most widely used asphalt modifiers, and extensive research has been conducted on it [7]. Behnood et al. found that SBS improves asphalt's rutting resistance at high temperatures [8]. Zhang et al. discovered that SBS improves the aging resistance of asphalt [9]. Lin et al. noted that SBS increases asphalt's crack resistance at low temperatures [10]. Gong et al. observed that SBS improves asphalt's resistance to oxidative damage [11]. However, a high dosage of SBS will not only reduce the workability of modified asphalt but also greatly increase its cost [12], which is bad for construction.

Many researchers have proposed using CR to partially replace SBS to reduce production costs [13]. CR is derived from ground waste tires [14]. Preparing asphalt using CR not only helps mitigate the environmental problems associated with waste tire disposal [15] but also significantly

* Corresponding author at: College of Civil Engineering & Transportation, South China University of Technology, Guangzhou, Guangdong 510640, China.
E-mail address: cthu@scut.edu.cn (C. Hu).

enhances the rutting resistance and fatigue resistance performance of asphalt [16]. To improve the modification effect of CR and enhance the storage stability of CR-modified asphalt, some researchers have pre-treated CR with aromatic-rich solvents [17,18]. Liu et al. found that the use of oils with high content of aromatic and naphthenic on the solubilization pretreatment of CR will enhance the content of lightweight components of CR-modified asphalt, reduce the rutting resistance and fatigue resistance of asphalt, and enhance the low-temperature cracking resistance of asphalt [17]. Huang et al. found that 1 hour pretreatment of CR using FEO shows a harmonious balance of rutting resistance, fatigue resistance, and low-temperature cracking resistance [19]. Zhang et al. found that the incorporation of CR with SBS can improve the elastic recovery ability of modified asphalt because of the crosslinking structure of CR [20]. Yang et al. found that the aging and fatigue resistance performance of CR/SBS-CMA is superior to that of asphalt modified with either SBS or CR alone [21]. Nan et al. discovered that CR/SBS-CMA has excellent fatigue resistance performance [22]. However, CR/SBS-CMA still suffers from the issue of poor workability [4]. This also means that when using CR/SBS-CMA for paving, a higher temperature is required, leading to increased energy consumption and more greenhouse gas emissions. Undoubtedly, this hinders the application of CR/SBS-CMA.

To address this issue, some researchers have employed warm mix additives to enhance the workability of CR/SBS-CMA [23,24]. Based on the process involved in temperature reduction, warm mix additives are classified into three groups: a) organic additives, b) foaming-based warm mix additives, and c) chemical additives [25]. The most commonly used to reduce the viscosity of modified asphalt is organic additives [3]. Considering that CR/SBS-CMA is more widely used in the south of China where the temperature is high in summer, attention should be paid to using the warm mix additive to enhance the rutting resistance and fatigue resistance performance of CR/SBS-CMA while decreasing its viscosity. The commonly used organic additives with such characteristics include Sasobit and Deurex [26]. Gao et al. showed that Sasobit has a better viscosity reduction effect than Deurex when the dosage is lower than 2.75 % [27]. Yang et al. found that the complex modulus of Sasobit warm-mixed asphalt is higher than that of Deurex, the melting point of Sasobit is lower than that of Deurex, and the dispersion effect of Sasobit in asphalt is better than that of Deurex [28]. Therefore, Sasobit is suitable as the warm mix additive in reducing the viscosity of CR/SBS-CMA. Sasobit, a synthetic Fischer-Tropsch wax derived from coal gasification, is commonly used as a warm mix additive for asphalt [29]. Its chemical formula is C_nH_{2n+2} [30]. Current studies on the CR/SBS-CMA with Sasobit were summarized in Table 1. Erkus et al. found that Sasobit can reduce the 135 °C viscosity of CR/SBS-CMA, which in turn lowers the construction temperature and decreases energy consumption [23]. Yue et al. discovered that adding Sasobit improves the rutting resistance of CR/SBS-CMA at high temperatures [31]. Lagos-Varas et al. found that Sasobit enhances the fatigue resistance performance of CR/SBS-CMA [24]. Yue et al. found that the addition of Sasobit can enhance the healing ability of the CR/SBS-CMA [32].

Overall, existing studies mainly focus on the effect of a certain content of Sasobit on high and medium-temperature rheological properties

of CR/SBS-CMA. The existing studies have insufficient ranges of Sasobit content and lack of focus on the effect of Sasobit content on the storage stability, viscosity, and full temperature range rheological properties of CR/SBS-CMA. These issues affect the application of CR/SBS-CMA containing Sasobit. To address these issues, this study delves deeply into the influence of Sasobit content on the rheological properties and storage stability of CR/SBS-CMA through various tests. Five types of CR/SBS-CMA with different Sasobit contents were prepared in this study. The Brookfield viscosity tests were used to measure the viscosity of asphalt samples. The Fourier transform infrared spectroscopy (FTIR) tests were conducted to study the modification mechanism. The cigar tube and fluorescence microscopy (FM) tests were employed to study the storage stability of asphalt samples. The penetration, softening point, and ductility of CR/SBS-CMA were assessed through conventional tests. The rheological behaviors of asphalt samples were assessed through a comprehensive series of tests, including temperature sweep, frequency sweep, multiple stress creep recovery (MSCR), linear amplitude sweep (LAS), and bending beam rheometer (BBR) tests.

2. Materials and testing methods

2.1. Materials

In this study, 70# asphalt produced by Shell was used as the virgin asphalt. Photographs of CR, SBS, and Sasobit are shown in Fig. 1. The 60 mesh CR derived from truck tires was produced using the mechanical shredding method, in which the CR chips were milled into finer particles at ambient temperature. The basic properties of the asphalt are shown in Table 2. The physical characteristics of CR, SBS, and Sasobit are shown in Table 3, Table 4, and Table 5, respectively.

2.2. Preparation of samples

CR pretreatment process and preparation process of CR/SBS-CMA are shown in Fig. 2. CR and furfural extraction oil (FEO) were mixed at ambient temperature and manually stirred for 1 minute. For the CR to fully absorb the FEO, the mixture from the previous step was then placed in an oven at 140 °C and kept for 1 hour. After that, it was filtered using filter paper to obtain pre-swelled CR. The virgin asphalt was heated to 180 °C and then pre-swelled CR and SBS were added. The obtained mixture was blended using a blender at a rotation speed of 600 rpm for 40 minutes at 180 °C. Then the mixture was sheared using a high-speed shearing machine at a rotation speed of 5000 rpm for 1 hour at 180 °C. Finally, Sasobit and sulfur were added to the obtained mixture and then blended using a blender at a rotation speed of 600 rpm for 2 hours at 180 °C. The CR/SBS-CMA sample without Sasobit was prepared using the same process to ensure that all samples in the experiment had the same aging level.

According to previous studies, the amounts of CR and SBS used in this research were determined to be 8 wt% and 3 wt%, respectively [19, 23]. Based on Sasol wax recommendations, Sasobit dosing below 0.8 wt % does not have a significant modification effect, while above 4 wt%, it significantly reduces the low-temperature performance of asphalt [33]. In this study, four Sasobit dosages of 1 wt%, 2 wt%, 3 wt%, and 4 wt% were used. The asphalt samples used in the experiment and their corresponding codes are shown in Table 6. The Rolling Thin Film Oven Test (RTFOT) and Pressurized Aging Vessel (PAV) test were used to simulate short-term aging and long-term aging. The RTFOT was conducted according to the ASTM D2872 and the PAV test was conducted according to the ASTM D6521.

2.3. Testing methods

A series of tests were conducted to comprehensively study the influence of Sasobit content on CR/SBS-CMA. The experimental scheme is illustrated in Fig. 3.

Table 1
Overview of studies on the CR/SBS-CMA with Sasobit.

Reference	Year	Sasobit content (wt %)	Testing method
Erkus et al. [23]	2020	2, 3, 4	Softening point test, Viscosity test, Temperature sweep test
Yue et al. [31]	2021	3	LAS test
Lagos-Varas et al. [24]	2023	2, 4	MSCR test, LAS test, BYET test
Yue et al. [32]	2023	2, 3, 4	SEM test, Frequency sweep test, LAS test, Time sweep test, Healing test

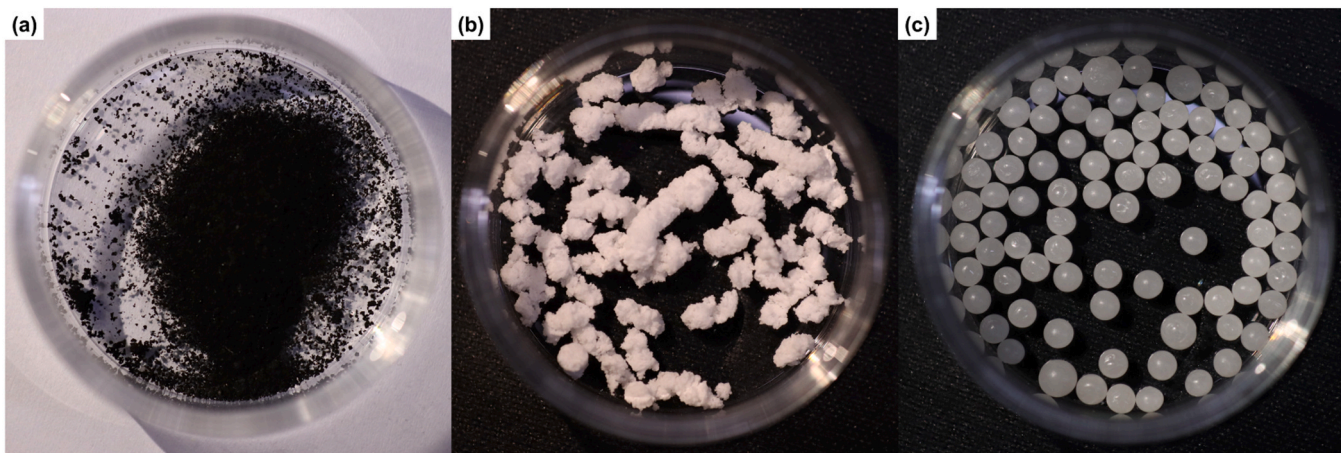


Fig. 1. CR (a), SBS (b), and Sasobit (c).

Table 2
Basic properties of the virgin asphalt.

Property	Value	Method
Penetration (25 °C, 0.1 mm)	67.7	ASTM D 5
Softening point (°C)	46.8	ASTM D 36
Ductility (15 °C, cm)	> 100	ASTM D 113
Density (15 °C, g/cm ³)	1.022	ASTM D 70
Solubility (trichloroethylene, %)	99.8	ASTM D 2042

Table 3
Physical characteristics of CR.

Property	Value
Rubber hydrocarbon (%)	52
Heating loss (%)	0.53
Ferric (%)	0.028
Total ash (%)	4.01
Particle size (mm)	0.23–0.27
Carbon black (%)	20

Table 4
Physical characteristics of SBS.

Property	Value
S/B ratio	30/70
Oil content (%)	0.70
Volatility (%)	1.00
Total ash (%)	0.20
Tensile strength (MPa)	18.0
Elongation (%)	700

Table 5
Physical characteristics of Sasobit.

Property	Value
Melting point (°C)	100
Flashing point (°C)	290
Viscosity (135 °C, Pa·s)	5.47×10^3
Viscosity (150 °C, Pa·s)	3.26×10^{-3}
Penetration (25 °C, 0.1 mm)	1.0
Penetration (60 °C, 0.1 mm)	8.0

2.3.1. Fourier transform infrared spectroscopy (FTIR) test

A Fourier transform infrared spectrometer (Nicolet iS50, Thermo Fisher Scientific, USA) was employed to analyze the functional groups in the samples, so as to evaluate their properties and modification

mechanism [34]. To compare the changes in functional groups of CR/SBS-CMA before and after the addition of Sasobit, asphalt samples without Sasobit (CR/SBS-0), asphalt samples with Sasobit (CR/SBS-4), and Sasobit were selected as samples for FTIR tests. The transmission mode was utilized, with a wavenumber range from 4000 to 400 cm⁻¹, a resolution of 4 cm⁻¹, and 32 scans conducted at ambient temperature [35].

2.3.2. Brookfield viscosity test

In this study, a Brookfield rotational viscometer was utilized to assess the viscosity-temperature properties of CR/SBS-CMA according to the ASTM D4402. The No. 27 spindle rotor was used for the tests, and the temperatures tested were 135 °C, 150 °C, 165 °C, 180 °C, and 195 °C. The tests were repeated three times, and the average values were taken as the final results.

2.3.3. Conventional tests

Conventional tests, including penetration tests (at 25 °C), softening point tests, and ductility tests (at 15 °C), are typically performed to assess the physical properties of CR/SBS-CMA samples. The penetration, softening point, and ductility tests were carried out according to the ASTM D5, ASTM D36, and ASTM D113 standards, respectively. All asphalts used in conventional tests were subjected to the RTFOT for 85 minutes to simulate short-term aging. Each test was repeated three times, and the average value was taken as the final result.

2.3.4. Dynamic shear rheometer (DSR) test

The dynamic shear rheometer (DSR) tests were conducted using a dynamic shear rheometer (Kinexus lab+, Malvern Panalytical, UK). In the high-temperature zone (above 40 °C), the samples were tested using parallel plates with a diameter of 25.0 mm and a gap of 1.0 mm. For temperatures below 40 °C, the samples were tested using parallel plates with a diameter of 8.0 mm and a gap of 2.0 mm. All asphalts were subjected to RTFOT for 85 minutes to simulate the short-term aging before the DSR tests according to ASTM D2872.

The temperature sweep (TS) tests were used to evaluate the viscoelastic properties of CR/SBS-CMA in the temperature range of 16–82 °C, and the rutting parameter ($G^*/\sin\delta$) was used to evaluate the high-temperature performance of CR/SBS-CMA. The temperature sweep tests were conducted based on ASTM D6373. The high-temperature range was set from 46 °C to 82 °C, with 6 °C increments, and a constant frequency of 1.59 Hz. For the low-temperature range, the experimental temperatures ranged from 16 °C to 34 °C, increasing by 3 °C increments. The temperature sweep tests were conducted at a constant frequency of 1.59 Hz and 1 % strain.

The frequency sweep (FS) tests were employed to evaluate the

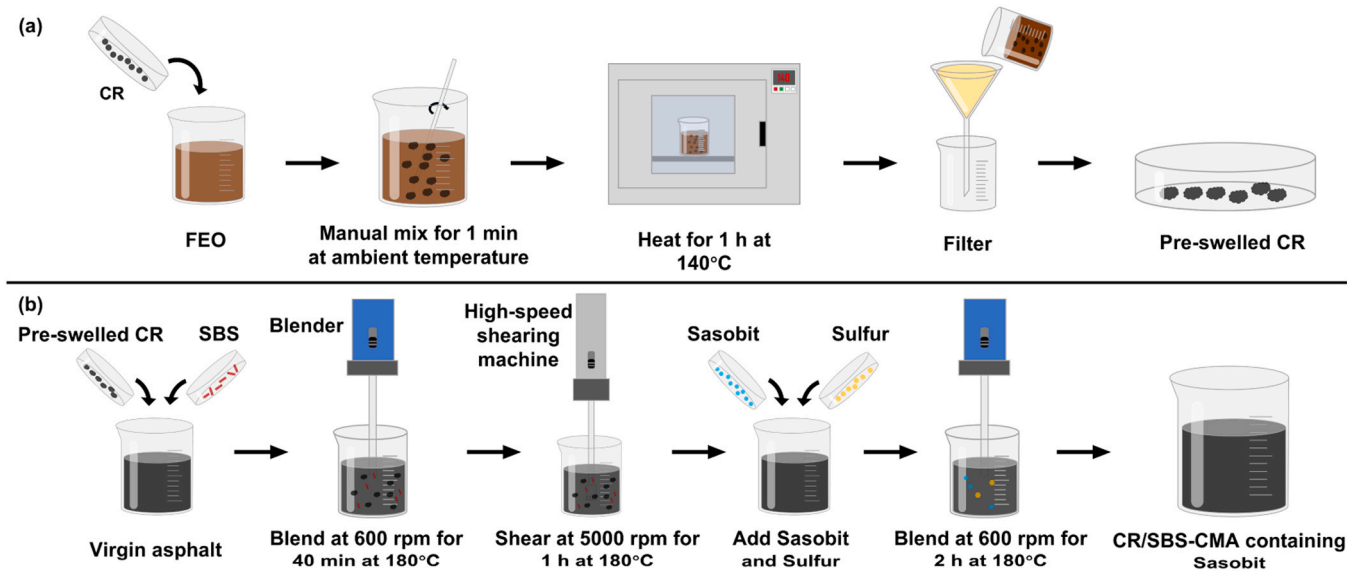


Fig. 2. CR pretreatment process (a) and preparation process of CR/SBS-CMA containing Sasobit (b).

Table 6

Asphalt samples and codes.

Asphalt sample	Code
8 wt% CR + 3 wt% SBS	CR/SBS-0
8 wt% CR + 3 wt% SBS + 1 wt% Sasobit	CR/SBS-1
8 wt% CR + 3 wt% SBS + 2 wt% Sasobit	CR/SBS-2
8 wt% CR + 3 wt% SBS + 3 wt% Sasobit	CR/SBS-3
8 wt% CR + 3 wt% SBS + 4 wt% Sasobit	CR/SBS-4

viscoelastic properties of asphalt samples over a wide range of temperatures and frequencies [36]. The strain amplitude in the tests was kept within the specimen's linear viscoelastic range. The tests were conducted at frequencies ranging from 0.1 Hz to 30 Hz and at temperatures of 4 °C, 16 °C, 28 °C, 40 °C, 52 °C, 64 °C, and 76 °C, respectively.

The multiple stress creep recovery (MSCR) tests were employed to accurately model the repeated loading and unloading of asphalt pavement at high temperatures, effectively reflecting the delayed elastic characteristics of high-viscosity asphalt [9]. The MSCR tests were conducted under stress-controlled mode according to ASTM D7405. The tests were performed in two stages: the first stage used a control stress of 0.1 kPa, and the second stage used a control stress of 3.2 kPa. Each loading cycle involved applying constant stress for 1 second, followed by recovery at zero stress for 9 seconds. The test comprised a total of 30 cycles, with the first 10 cycles at a stress level of 0.1 kPa used to condition the sample without recording data, the next 10 cycles at 0.1 kPa for data collection, and the final 10 cycles at 3.2 kPa for data collection. The results were used to calculate non-recoverable creep compliance (J_{nr}), percentage recovery (R), the difference in non-recoverable creep compliance ($J_{nr\ diff}$), and the difference in percentage recovery (R_{diff}). The tests were repeated three times, and the average values were taken as the final results.

The linear amplitude sweep (LAS) tests were conducted in a strain-controlled mode with a test temperature of 20 °C. The LAS tests were performed in two phases: The first stage was a frequency sweep, where the DSR swept the asphalt sample at a frequency range of 0.2–30 Hz at 0.1 % strain amplitude. The second stage was an amplitude sweep, during which the DSR was used to increase the strain amplitude from 0.1 % to 30 % at a constant frequency (10 Hz) for a sweep time of 300 s [37]. Each test was repeated three times, and the average fatigue life was taken as the final fatigue life.

2.3.5. Bending beam rheometer (BBR) test

The low-temperature performance of CR/SBS-CMA samples was assessed using the BBR test. According to ASTM D 6648, CR/SBS-CMA samples, after undergoing RTFOT and PAV tests, were molded into beams measuring 127 mm × 6.35 mm × 12.7 mm. A constant load of 980 mN ± 50 mN was applied for 240 seconds at temperatures of -12 °C, -18 °C, and -24 °C. The creep stiffness (S) and creep rate (m-value) were recorded at the 60-second mark. These values were used to evaluate the stiffness and susceptibility of asphalt to thermal cracking at low temperatures [38]. Each test was repeated three times, and the average value was taken as the final result.

2.3.6. Cigar tube test

The cigar tube test can be used to evaluate the storage stability of modified asphalt. According to ASTM D7173, cigar tubes containing different CR/SBS-CMA samples were heated at 163 °C for 48 hours. After heating, the cigar tubes were placed in a refrigerator for 4 hours and then evenly divided into three parts. For each CR/SBS-CMA sample, the softening points from the top and bottom parts were measured, and the softening point difference (SPD) was calculated [39]. The tests were repeated three times, and the average values were taken as the final results.

2.3.7. Fluorescence microscopy (FM) test

A fluorescence microscope (Leica DMi8) was used to observe the micrographs of different segment specimens from the cigar tubes. After the cigar tube tests, CR/SBS-CMA samples from the top and bottom parts of the tubes were prepared as microscopic samples [19]. The asphalt was dripped onto a glass slide and covered with a coverslip to prepare the microscopic sample. Once the micrographs were obtained, Photoshop's color selection tool was used to select and count the number of pixels occupied by SBS and CR respectively in the micrographs [40]. Area ratio (AR) was defined as the percentage of SBS's (or CR's) pixels to the total number of pixels in a photo, which was calculated according to Eq. (1):

$$AR = \frac{N_{add}}{N_{total}} \times 100 \% \quad (1)$$

Where: AR represents the area ratio of a photo, N_{add} represents the number of SBS's (or CR's) pixels in the photo, and N_{total} represents the total number of photo's pixels.

Four photos were taken of each sample from the top and bottom of the cigar tube, and the AR was calculated for each photo. The area ratio

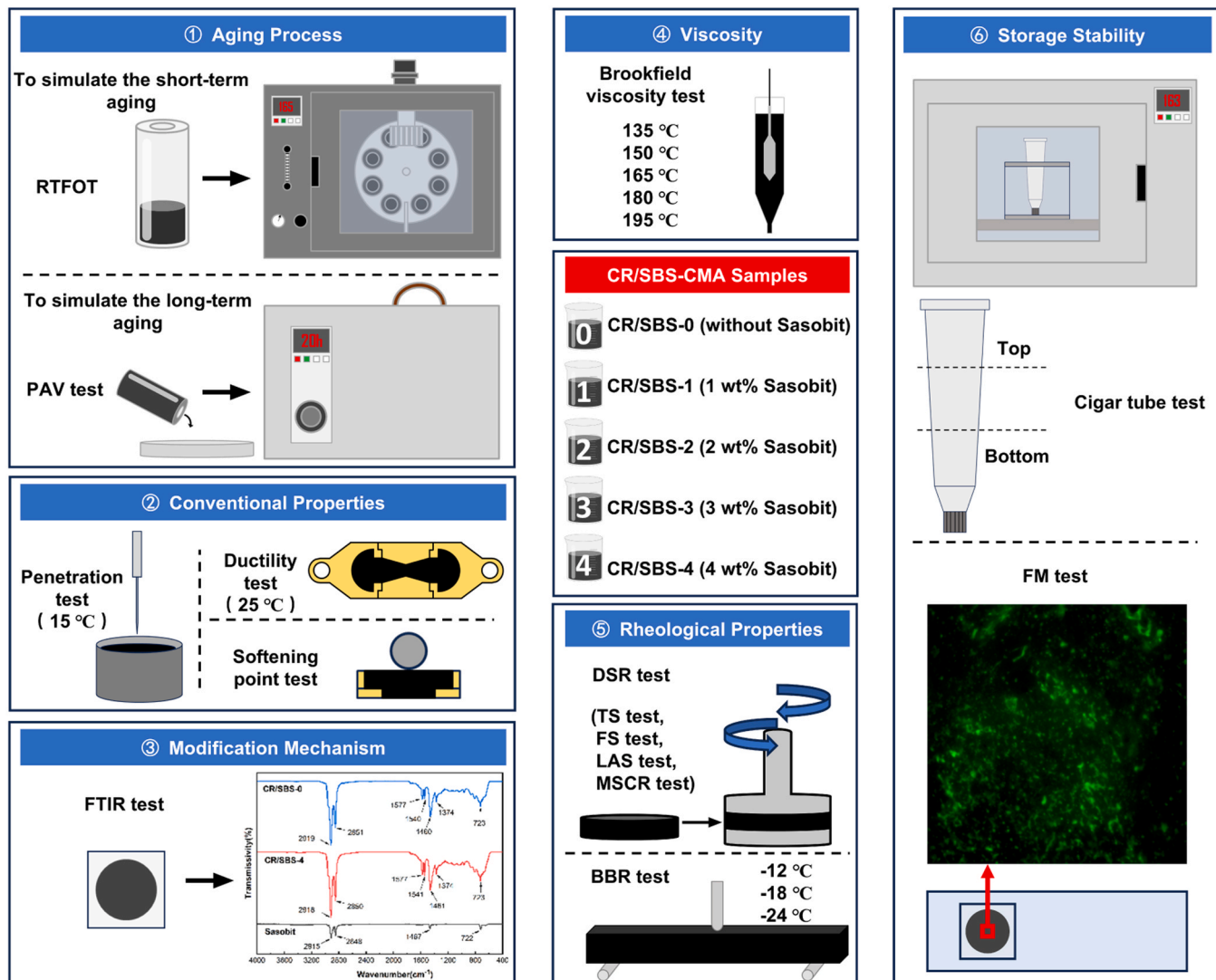


Fig. 3. Experimental scheme.

difference (ARD) was calculated according to Eq. (2):

$$ARD = |\overline{AR}_{top} - \overline{AR}_{bottom}| \quad (2)$$

Where: ARD represents the area ratio difference of a sample, \overline{AR}_{top} represents the average value of AR from the top part of the cigar tube of the sample, and \overline{AR}_{bottom} represents the average value of AR from the bottom part of the cigar tube of the sample.

3. Result and discussion

3.1. Brookfield viscosity tests analysis

Viscosity reflects the internal frictional resistance between molecules during fluid flow, it determines the workability of asphalt and has a decisive influence on the construction temperature [41]. The results of the Brookfield viscosity test are shown in Fig. 4. At 135 °C, the viscosity of CR/SBS-0 is 2.89 Pa·s, while the viscosity of CR/SBS-1 and CR/SBS-4 is 2.69 Pa·s and 1.91 Pa·s, respectively. Compared to CR/SBS-0, the viscosity of the latter two decreases by 10 % and 33.9 %. At 195 °C, their viscosity decreases by 15 % and 44 % compared to CR/SBS-0. The viscosity of CR/SBS-4 decreased by 72.6 % and 81.1 % at 150 °C and 180 °C, respectively, compared to CR/SBS-CMA without Sasobit in the results of Liu et al. [42]. Overall, in the temperature range of 135 °C to 195

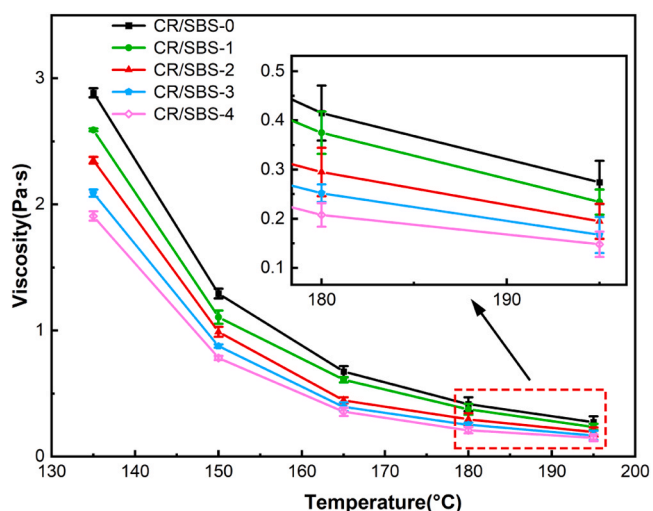


Fig. 4. Brookfield viscosity test results.

°C, the addition of Sasobit can significantly reduce the viscosity of CR/SBS-CMA, with higher Sasobit content leading to a more pronounced reduction in viscosity. This effect is attributed to the fact that Sasobit has a melting point close to 100 °C and fully dissolves in the asphalt at temperatures above 116 °C [43]. The longer chains of Sasobit will help it to dissolve in the asphalt, thereby reducing the asphalt's viscosity [44]. Lower viscosity indicates better workability, allowing for reduced mixing and compaction temperatures, which in turn reduces energy consumption during construction. The addition of Sasobit can decrease the viscosity of CR/SBS-CMA, and improve its workability.

3.2. FTIR analysis

The FTIR test results are presented in Fig. 5. The locations of the characteristic peaks and the IR absorption of the relevant functional groups are listed in Table 7.

The absorption peaks at 2921 cm⁻¹ and 2850 cm⁻¹ correspond to the stretching of -CH₂ and -CH₃ groups respectively. Peaks between 1640 and 1540 cm⁻¹ represent conjugated double bonds C=C and C=O. Peaks around 1460 cm⁻¹ are associated with the -CH₃, -CH₂, and -CH stretching vibrations. The peak at 1374 cm⁻¹ corresponds to -CH₃ bending (aliphatic), while the peak at 722 cm⁻¹ is related to the -C-H stretching of a benzene ring.

It can be observed that Sasobit shows characteristic peaks at 2915 cm⁻¹, 2848 cm⁻¹, 1467 cm⁻¹, and 722 cm⁻¹, indicating the presence of methylene groups. Additionally, the characteristic peaks of both CR/SBS-0 and CR/SBS-4 overlap, suggesting that the position of these peaks remains unchanged after the addition of Sasobit. This implies that no significant chemical reactions have occurred. Therefore, the reduction in viscosity after the addition of Sasobit to CR/SBS-CMA is primarily a physical process.

3.3. Conventional tests analysis

The results of penetration, softening point, and ductility are illustrated in Fig. 6. From Fig. 6(a), it can be observed that the penetration at 25 °C of CR/SBS-CMA decreases with the increase of Sasobit content. The penetration of CR/SBS-0 is 60.0 mm, and that of CR/SBS-4 is 41.4 mm, which is 31 % lower than the former. The penetration of CR/SBS-4 decreased by 16.9 % compared to CR/SBS-CMA without Sasobit, according to Qian et al. [45]. These indicate that the addition of Sasobit can enhance the toughness of the CR/SBS-CMA. However, the penetration of CR/SBS-4 is below 45 mm, making it more prone to cracking at lower temperatures. This is because Sasobit has a melting point of

Table 7
Peaks and assignments for the FTIR wavenumber.

Wavenumber (cm ⁻¹)	Functional group
2921	-CH ₂ stretching
2850	-CH ₃ stretching
1640–1540	Conjugated double bonds C=C and C=O
1460, 1461, 1467	-CH ₃ , -CH ₂ , -CH stretching vibration
1374	-CH ₃ bending (aliphatic)
722, 723	-C-H benzene ring

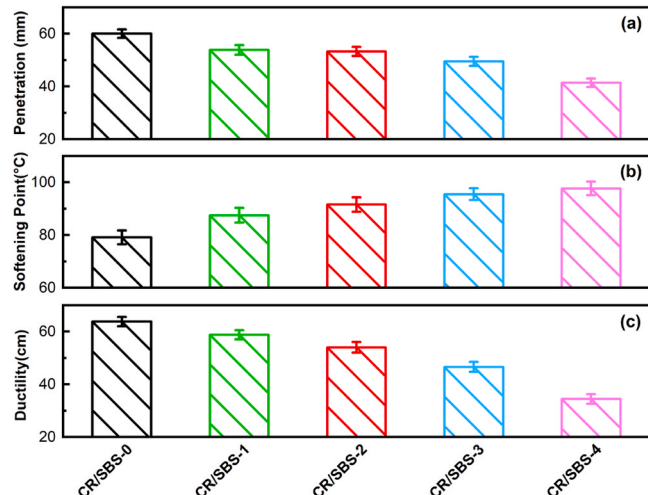


Fig. 6. Results of conventional tests: (a) penetration (25 °C), (b) softening point, and (c) ductility (15 °C).

around 110 °C and remains solid at temperatures below this point, forming a two-phase composite structure with the asphalt [46]. Since Sasobit is solid at 25 °C, both the asphalt phase and Sasobit share the load when the material is under compressive stress, leading to an increase in compressive strength, which is observed as an increase in penetration.

From Fig. 6(b), it can be seen that the softening point of CR/SBS-CMA increases with the increase of Sasobit content, and the softening point of CR/SBS-4 is increased by 8.6 °C compared with that of CR/SBS-0. The softening point of CR/SBS-4 decreased by 36.7 °C compared to that of CR/SBS-CMA without Sasobit doping according to Qian et al. [45]. These suggest that the incorporation of Sasobit can improve the high-temperature performance of CR/SBS-CMA. This is because the melting point of Sasobit is about 110 °C, which forms a lattice structure in asphalt binder at temperatures lower than the melting point and provides better stability, thus increasing the softening point of CR/SBS-CMA [33].

From Fig. 6(c), it can be seen that the ductility of CR/SBS-CMA at 15 °C decreases dramatically with the increase of Sasobit content. The ductility of CR/SBS-4 is 343.8 mm, which is nearly 300 mm lower than that of CR/SBS-0 (637.5 mm), indicating that the addition of Sasobit will make the asphalt more susceptible to cracking at lower temperatures. Since Sasobit is solid at 15 °C, the tensile stress causes stress to concentrate in the asphalt phase, leading to a reduction in the resistance of tensile strength. This is manifested by the decreased ductility observed at 15 °C.

3.4. Temperature sweep analysis

Fig. 7 presents the complex modulus (G^*) and phase angle (δ) of the CR/SBS-CMA samples. As shown in Fig. 7(a), the G^* of the asphalt samples increases with the increase of Sasobit content, particularly at temperatures below 40 °C. This indicates that the addition of Sasobit can

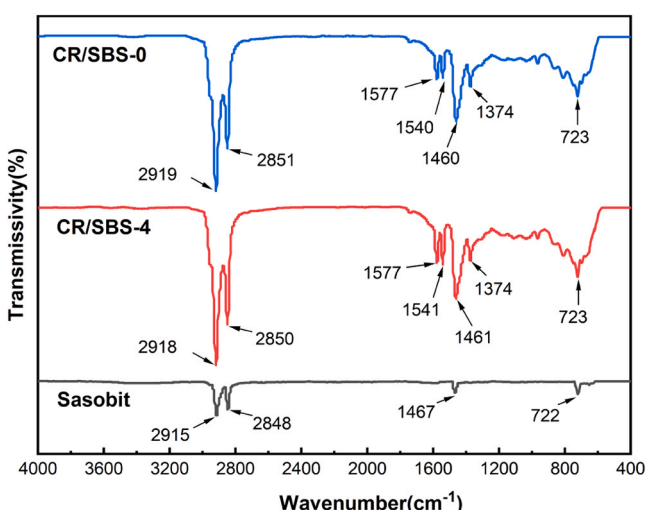


Fig. 5. FTIR test results.

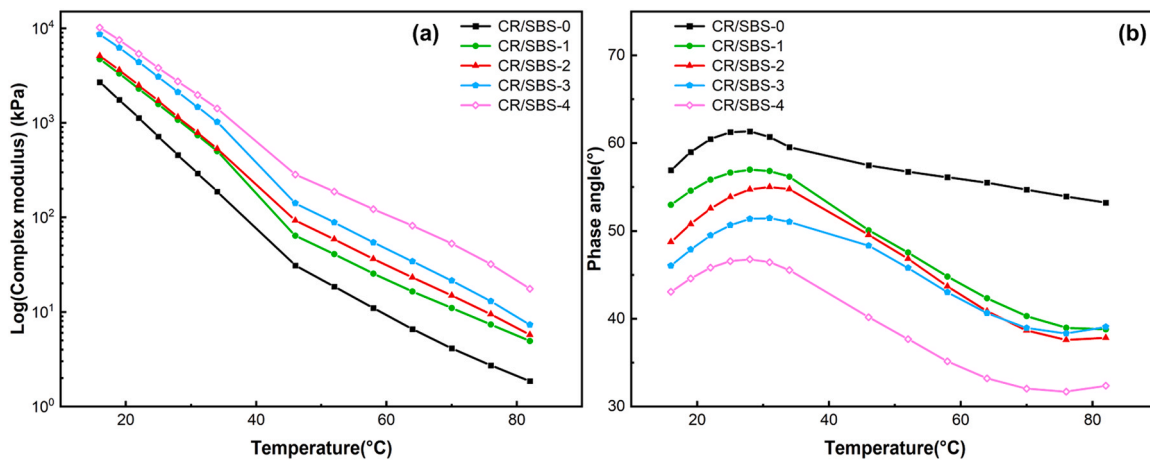


Fig. 7. The results of the temperature sweep test: (a) complex modulus (G^*) curves, and (b) phase angle (δ) curves.

enhance the hardness of the CR/SBS-CMA, with the effect being more pronounced at lower temperatures. According to Fig. 7(b), the phase angle of the CR/SBS-CMA samples decreases as the Sasobit content increases, with this trend being more pronounced at higher temperatures. These observations suggest that the addition of Sasobit can improve the elasticity of CR/SBS-CMA, particularly in the 46 °C - 76 °C range. However, as the temperature rises further above the softening point of the asphalt, the material becomes more viscous, causing the effect of Sasobit on enhancing elasticity to gradually diminish.

Furthermore, it can be seen in Fig. 7(b) that the phase angle of CR/SBS-CMA at 16–82 °C shows two phases. In the first stage, the phase angle increases rapidly with increasing temperature. At this stage, because of the low temperature, the base asphalt, which accounts for the largest proportion of the modified asphalt, is hard, so it dominates the mechanical properties of CR/SBS-CMA. As the temperature increases, the asphalt softens rapidly and the phase angle increases rapidly with it. In the second stage, as base asphalt continues to soften until the viscosity of it being low enough to allow the CR particles and elastic network of the polymer to influence the mechanical properties of the modified binders [47], the phase angle of modified asphalt begins to decrease with the increase of temperature.

Based on the temperature sweep test results, the rutting parameter ($G^*/\sin\delta$), which is commonly used to evaluate high-temperature performance [48], is calculated and shown in Fig. 8. A higher $G^*/\sin\delta$ value generally indicates better high-temperature performance of the

asphalt [9]. As observed in Fig. 8, within the temperature range of 16–82 °C, the $G^*/\sin\delta$ value increases with the addition of Sasobit. At 82 °C, the $G^*/\sin\delta$ values of CR/SBS-CMA with 1 %, 2 %, 3 %, and 4 % Sasobit content exceed the required 2.2 kPa. When compared to CR/SBS-0 without Sasobit, their $G^*/\sin\delta$ values increase by 140 %, 204 %, 301 %, and 1216 %, respectively. This demonstrates that Sasobit can enhance the high-temperature performance of CR/SBS-CMA, with the 4 % Sasobit content providing the most substantial improvement.

3.5. Frequency sweep analysis

The complex modulus master curve (with a reference temperature of 40 °C) is established by applying the Williams–Landel–Ferry (WLF) Time-Temperature superposition principle and the Sigmoidal Model, as presented in the following equations [49] :

$$\log\alpha_T = \frac{-C_1(T - T_0)}{C_2 + (T - T_0)} \quad (3)$$

$$\log f_R = \log f + \log\alpha_T = \log f + \frac{-C_1(T - T_0)}{C_2 + (T - T_0)} \quad (4)$$

$$\log(G^*) = \delta + \frac{\alpha}{1 + e^{\beta + \gamma \log f_R}} \quad (5)$$

Where: α_T represents the shift factor, T represents the measured temperature (°C), C_1

and C_2 are constants, T_0 represents the reference temperature (°C), f_R represents the replaced frequency (Hz), f represents the measured frequency (Hz), G^* represents the complex modulus (Pa), δ , α , β and γ are coefficients.

ZSV was estimated through extrapolation from the complex viscosity curve that was fitted by the simplified Cross model [50], with the application in Eq. (6):

$$\eta^* = \frac{\eta_0^*}{1 + (2\pi f K)^m} \quad (6)$$

Where: η_0^* represents the ZSV (Pa·s), η^* represents the complex viscosity (Pa·s), f represents the frequency (Hz), K and m are constants.

The master curves of the CR/SBS-CMA samples, with a reference temperature of 40 °C, are constructed over a wide range of frequencies, as shown in Fig. 9. It can be seen in Fig. 9 that in the low-frequency (high-temperature) region, the complex modulus of CR/SBS-CMA increases significantly with the increase of Sasobit content, and there is no significant change in the phase angle, which suggests that the addition of Sasobit can enhance the high-temperature properties of CR/SBS-CMA significantly [9]. In the high-frequency (low-temperature) region,

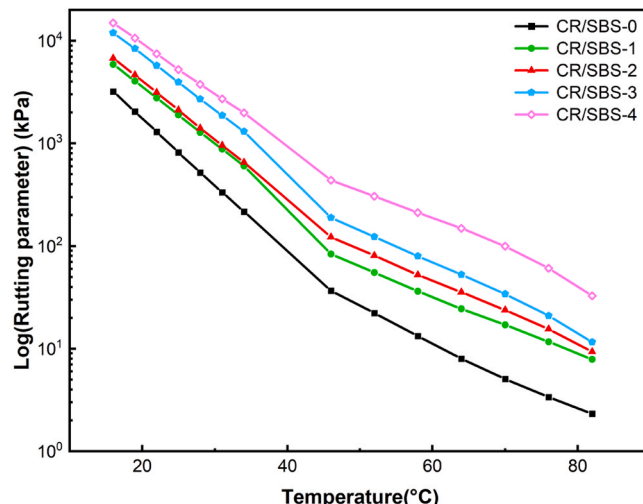


Fig. 8. Rutting parameter ($G^*/\sin\delta$) curves.

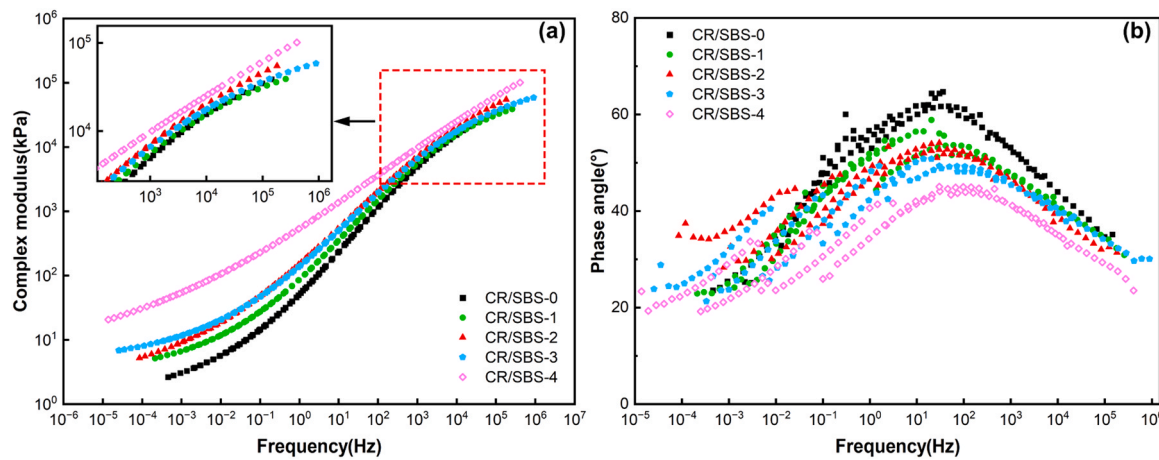


Fig. 9. Complex shear modulus (G^*) master curves (a) and phase angle (δ) master curves (b).

Sasobit did not significantly improve the complex modulus of CR/SBS-CMA, but significantly reduced the phase angle, which also showed that Sasobit made CR/SBS-CMA brittle at low temperatures. This will have a negative impact on the low-temperature performance of CR/SBS-CMA, which is also reflected in the ductility test results. This is also because Sasobit is in a solid state at a temperature lower than the melting point, which makes CR/SBS-CMA hard and strengthens the elastic response, which is manifested in the increase of complex modulus and the decrease of phase angle. However, at the low temperature represented by high frequency, the CR/SBS-CMA itself has a high complex modulus and low phase angle, which makes the modification effect of Sasobit no longer obvious.

As observed in Fig. 9(b), the phase angle curves of the CR/SBS-CMA samples initially increase and then decrease with frequency, forming single peaks. This means that the phase angle increases and then decreases from low temperature to high temperature, which is the result of the combined effect of the additives and asphalt CR/SBS-CMA, as explained in Section 3.4.

3.6. MSCR tests analysis

To comprehensively evaluate the high-temperature rheological properties, the MSCR test was conducted. The results of R , J_{nr} , $J_{nr\ diff}$, and R_{diff} are presented in Fig. 10. J_{nr} represents the rutting resistance of the binder, and a higher J_{nr} value means lower rutting performance [51]. From Fig. 10, it can be seen that the J_{nr} values of the CR/SBS-CMA samples tend to decrease with the increase of Sasobit content. At both

0.1 kPa and 3.2 kPa, the J_{nr} of CR/SBS-4 is the lowest among the five samples, decreasing by 39 % and 35 % compared to CR/SBS-0, respectively. Compared with the research results of M. Lagos-Varas et al. [24], the J_{nr} of CR/SBS-CMA with 8 wt% CR and 3 wt% SBS was increased by 3 times and 1 time at 0.1kPa and 3.2kPa respectively after adding 4 wt% Sasobit. The addition of Sasobit can enhance the high-temperature rutting resistance of CR/SBS-CMA, which is consistent with the conclusions drawn from the temperature and frequency sweep tests.

R is an indicator used to assess the delayed elastic behavior of the binder, and a higher R -value means better recovery performance [51]. As shown in Fig. 10, the R -values of the CR/SBS-CMA samples tend to increase with the increase of Sasobit content. Similarly, CR/SBS-4 exhibits the highest R values at both 0.1 kPa and 3.2 kPa, with increases of 19 % and 9 % compared to CR/SBS-0, respectively. Compared with the research results of M. Lagos-Varas et al. [24], the R of CR/SBS-CMA with 8 wt% CR and 3 wt% SBS decreased by 80 % and 76 % respectively at 0.1kPa and 3.2kPa after adding 4 % Sasobit. These indicate that the addition of Sasobit can improve the recovery performance of CR/SBS-CMA.

The above phenomena are due to the fact that Sasobit forms a lattice structure in the asphalt at temperatures below its melting point and provides better stability [33], which increases the complex shear modulus and decreases the phase angle [52], therefore making the modified asphalt harder and increases the proportion of elastic deformations in the total deformation [28]. As a result, the rutting resistance and recovery performance of CR/SBS-CMA are improved.

Higher $J_{nr\ diff}$ and R_{diff} values indicate greater stress sensitivity in the

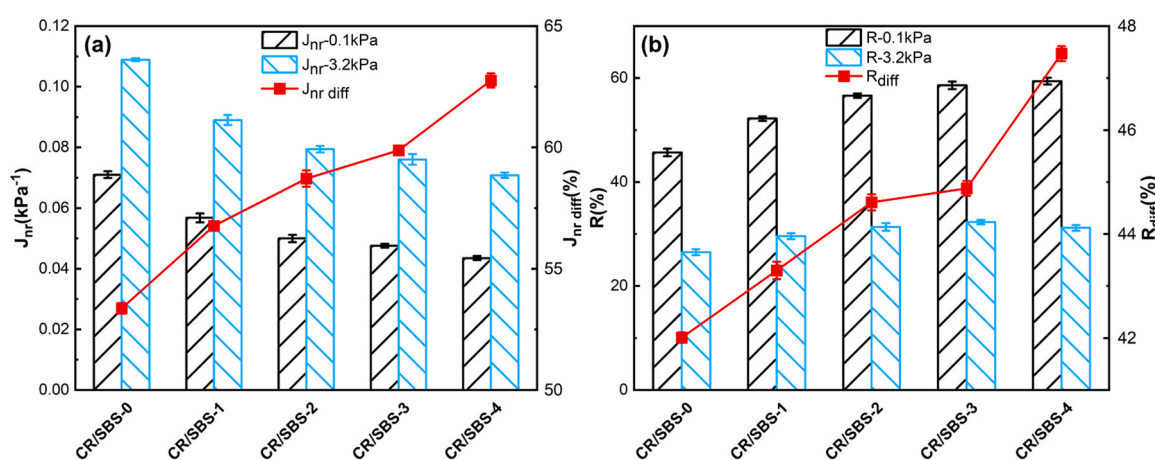


Fig. 10. MSCR test results of 0.1 kPa and 3.2 kPa at 64 °C: (a) J_{nr} and $J_{nr\ diff}$, (b) R and R_{diff} .

asphalt binder [53]. As the Sasobit content increases, both J_{nr} and R_{diff} continue to rise, reaching their maximum values when the Sasobit content reaches 4 %. This suggests that the addition of Sasobit can elevate the stress sensitivity of the CR/SBS-CMA samples.

3.7. LAS tests analysis

In this study, the LAS tests were used to evaluate the fatigue resistance performance of CR/SBS-CMA samples. Fig. 11(a) presents the stress-strain curves obtained from the LAS tests. It is evident that as the strain increases, the stress in each sample initially rises and then decreases, forming a stress peak. The strain and stress corresponding to the failure points of different asphalt samples, determined at the peak, are listed in Table 8. The magnitude of this peak indicates the hardness of the asphalt [22]. As shown in Table 8, as the Sasobit content increases, the stress peak value rises, indicating that Sasobit can enhance the hardness of the CR/SBS-CMA. Additionally, from Fig. 11(a), it is observed that CR/SBS-0 has the lowest peak stress, and after the peak, the stress decreases gradually with increasing strain. On the other hand, CR/SBS-4 exhibits the highest stress peak, but the stress rapidly decreases after the peak as the strain increases. The rate of decline is significantly higher than that of CR/SBS-3, indicating that the fatigue failure process in CR/SBS-4 progresses faster than in CR/SBS-3 at higher strain levels. The results suggest that the addition of Sasobit can increase the hardness of CR/SBS-CMA, enhancing its ability to resist fatigue failure at low strain levels. However, when the Sasobit content exceeds 4 %, it may negatively impact the asphalt's ability to resist fatigue failure at high strain levels. This effect may be attributed to the presence of Sasobit in a solid state below its melting point (approximately 110 °C), forming a two-phase structure with the asphalt. Once the critical strain is exceeded, the solid Sasobit within the asphalt fractures, leading to a rapid decline in the fatigue resistance performance of CR/SBS-CMA.

Using the S-VECD theory, the fatigue life of each CR/SBS-CMA sample was calculated at strain levels of 2.5 %, 5 %, and 15 %. The results are shown in Fig. 11(b). As illustrated in Fig. 11(b), at a strain level of 2.5 %, the fatigue life of CR/SBS-4 increases by 175.3 % compared to CR/SBS-0. However, at a strain level of 5 % and 15 %, the fatigue life of CR/SBS-4 increases by 76.8 % and 93.9 % compared to CR/SBS-0, respectively. Compared with the research results of M. Lagos-Varas et al. [24], the fatigue life of CR/SBS-CMA without Sasobit is increased by 7.1 times at 2.5 % strain and 1.4 times at 5 % strain after adding 4 % Sasobit. The results of Yue et al. showed that 3 % Sasobit doping at a high strain level of 9 % increased the fatigue life of CR/SBS-CMA by a factor of 3.1 compared to CR/SBS-CMA without Sasobit doping [31]. The results of LAS tests at 20 °C by M. Lagos-Varas et al. also showed that the fatigue resistance of CR/SBS-CMA still

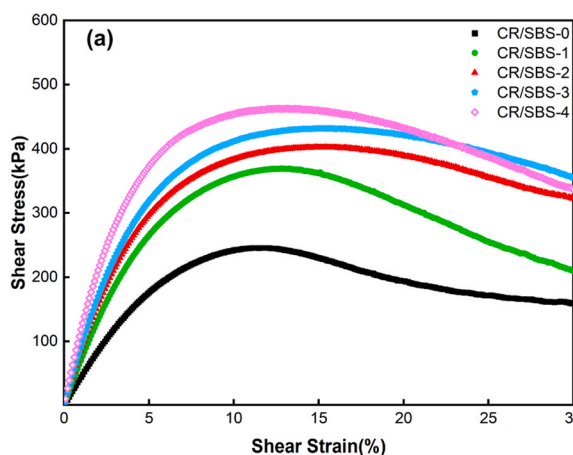


Table 8
Failure points in LAS tests.

Sample	Strain (%)	Peak stress (kPa)
CR/SBS-0	11.6	245.9
CR/SBS-1	12.7	369.3
CR/SBS-2	15.4	402.4
CR/SBS-3	15.2	431.6
CR/SBS-4	15.2	458.9

improves with the increase of Sasobit doping at a high strain level of 10 % [24]. Combined with the results of conventional tests, it can be seen that the addition of Sasobit has substantially improved the fatigue resistance performance of CR/SBS-CMA by stiffening it. This results in the excellent fatigue resistance performance of CR/SBS-CMA with different Sasobit dosages even at a high strain level of 15 %. However, in conjunction with the results of MSCR tests, it can be seen that the addition of Sasobit also makes CR/SBS-CMA more brittle, which is specifically shown as the enhancement of CR/SBS-CMA fatigue resistance performance by the increase in Sasobit doping is not as pronounced as at low strain levels under the larger loading represented by the 15 % strain level.

Overall, the addition of Sasobit can significantly enhance the fatigue life of CR/SBS-CMA at low strain levels. However, the addition of Sasobit makes the asphalt brittle, so when CR/SBS-CMA with Sasobit is subjected to high strain levels, the improvement in fatigue resistance performance becomes less pronounced. This suggests that Sasobit is more suitable for enhancing the fatigue resistance performance of CR/SBS-CMA pavement under lower traffic loads.

3.8. BBR tests analysis

The BBR test results at -12 °C, -18 °C, and -24 °C are presented in Fig. 12. Creep stiffness (S) and creep rate (m) are commonly used indicators to assess the low-temperature performance of asphalts [54]. A higher S value signifies greater tensile stress, while a lower m value indicates reduced stress relaxation [55]. Superior low-temperature rheological properties in asphalt are characterized by lower creep stiffness and higher creep rate [56]. According to AASHTO R 29, the low-temperature performance of CR/SBS-CMA is quantified using the criteria $m > 0.3$ and $S < 300$ MPa.

At -12 °C, -18 °C, and -24 °C, increasing the Sasobit content leads to an increase in the creep stiffness and a decrease in the creep rate of the CR/SBS-CMA samples. At all three temperatures, CR/SBS-4 exhibits the highest S value and the lowest m value. CR/SBS-2 at -24 °C, and CR/SBS-3 and CR/SBS-4 at -18 °C and -24 °C, fail to meet the standard criteria of $m > 0.3$ and $S < 300$ MPa. The S-value of CR/SBS-4 increased

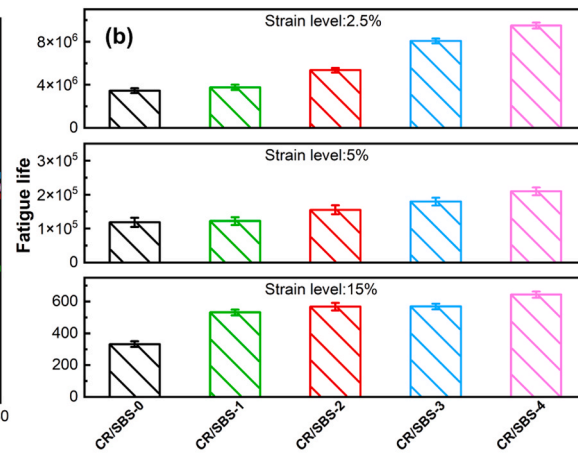


Fig. 11. Results of LAS test: (a) stress versus strain curves, (b) fatigue lives under different strain levels.

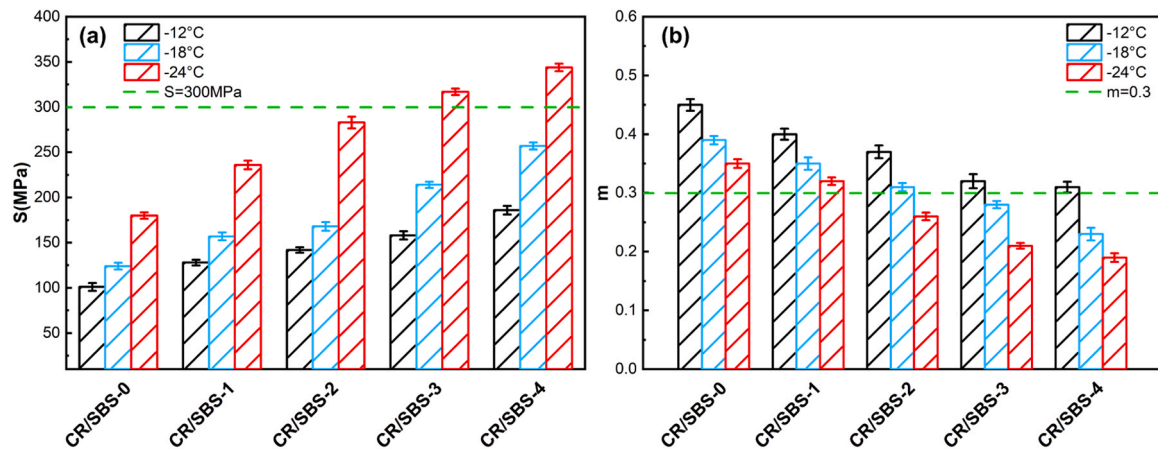


Fig. 12. BBR test results: (a) creep stiffness (S), (b) creep rate (m).

by 98.7 % and 34.3 % at -12°C and -18°C , respectively, and the m -value decreased by 39.6 % and 58.3 % at -12°C and -18°C , respectively, compared with the results of CR/SBS-CMA undoped with Sasobit in Liu et al. [42]. The addition of Sasobit raises the tensile stress in the CR/SBS-CMA while reducing stress relaxation. This indicates that Sasobit can decrease the low-temperature performance of the CR/SBS-CMA. This is because the addition of Sasobit increases the stiffness of CR/SBS-CMA at low temperatures, which leads to a decline in its low-temperature crack resistance [57]. CR/SBS-3 and CR/SBS-4 have poor low-temperature performance and are not suitable for use in areas with low winter temperatures.

3.9. Storage stability analysis

The results of the cigar tube test are shown in Fig. 13. The SPD effectively indicates the storage stability of CR/SBS-CMA, with a value of less than 2.5°C after 48 hours of heating indicating optimal stability [58]. It can be observed that as the Sasobit content increases, the SPD of the CR/SBS-CMA decreases. Specifically, the SPD for CR/SBS-3 and CR/SBS-4 are both below 2.5°C , representing a reduction of 1.8°C and 2.9°C compared to CR/SBS-0, respectively. This improvement in the SPD indicates that the addition of Sasobit can enhance the storage stability of CR/SBS-CMA from a mechanical perspective.

The micrographs of the top and bottom of CR/SBS-CMA samples from the cigar tubes were observed to determine the distributions of SBS and CR. Fig. 14 shows a set of micrographs of the CR/SBS-2 sample after

the cigar tube test. In Fig. 14 (a) and Fig. 14(b), the regions emitting green fluorescence are SBS, while the black areas represent non-fluorescent components such as asphalt and CR. In Fig. 14 (c) and Fig. 14 (d), the regions appearing black under visible light due to opacity are CR particles, whereas the red regions represent transparent components such as asphalt and SBS.

The results of the AR and ARD calculations are shown in Fig. 15. It is evident that after the cigar tube tests, the CR/SBS-CMA experienced varying degrees of segregation. Fig. 15 (a) illustrates that SBS, being less dense than asphalt, is more concentrated at the top and less at the bottom. Conversely, Fig. 15 (b) shows that CR, being denser than asphalt, is distributed oppositely to SBS. The ARD of both SBS and CR decreases with increasing dosage of Sasobit. The ARD of SBS and CR for CR/SBS-4 are 3.87 % and 18.67 %, respectively, which are 3.81 % and 11.31 % lower compared to 7.68 % and 29.98 % for CR/SBS-0, respectively. Overall, the addition of Sasobit can improve the segregation of SBS and CR within the asphalt, providing microscopic evidence that Sasobit positively impacts the storage stability of CR/SBS-CMA.

4. Conclusion

In this study, various tests were conducted to examine the influence of Sasobit content on the rheological properties and storage stability of CR/SBS-CMA. The results of the study will provide a method to reduce energy consumption and greenhouse gas emissions during the construction of CR/SBS-CMA pavements and provide a reference for the engineering application of CR/SBS-CMA. Based on the experimental results, the following conclusions can be drawn:

- The Brookfield viscosity tests demonstrated that Sasobit can effectively reduce the viscosity of CR/SBS-CMA within the temperature range of 135°C to 175°C . The FTIR test results indicated that this viscosity reduction process is a physical process.
- The correlation between Sasobit content and high-temperature rheological properties was analyzed using parameters such as softening point, rutting parameter, J_{nr} , and R . The results showed that the addition of Sasobit can improve the rutting resistance of CR/SBS-CMA. This indicates that CR/SBS-CMA pavements with Sasobit incorporated are very suitable for paving in high-temperature areas.
- Results from the LAS test confirmed that Sasobit can enhance the fatigue resistance performance of CR/SBS-CMA at low strain levels. However, when the strain level is higher than 5 %, adding Sasobit has little improvement in the fatigue life of CR/SBS-CMA. Considering the higher cost of Sasobit, the practice of improving the fatigue resistance of CR/SBS-CMA pavements by adding Sasobit is not suitable for heavy-loaded pavements.

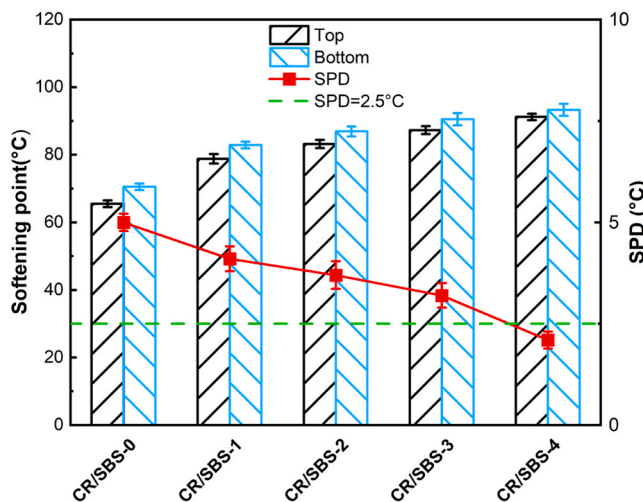


Fig. 13. Cigar tube test results.

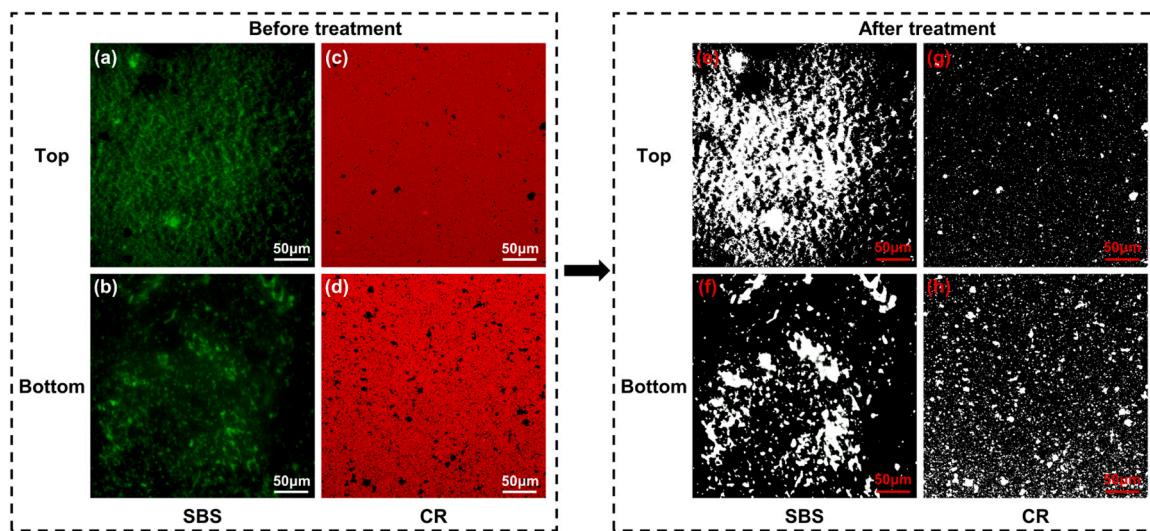


Fig. 14. Schematic diagram of the micrograph processing process of CR/SBS-CMA samples after cigar tube test.

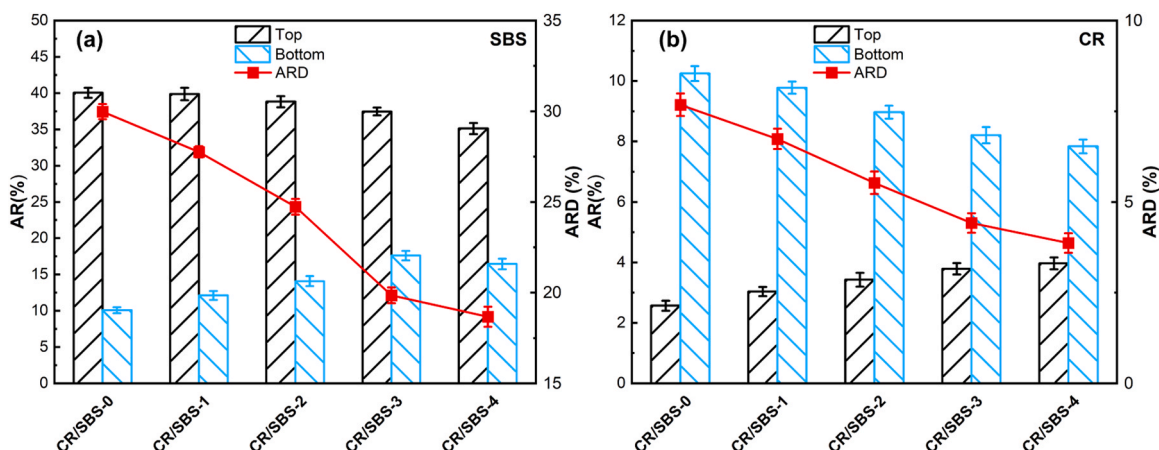


Fig. 15. The results of the micrograph analysis.

- (d) The BBR test results indicated that Sasobit will decrease the low-temperature cracking resistance of CR/SBS-CMA. In areas with low winter temperatures, the dosage of Sasobit should be lower than 3 %.
- (e) The cigar tube and FM test results provided evidence from both mechanical and microstructural perspectives that Sasobit will improve the storage stability of CR/SBS-CMA. This will effectively reduce losses due to CR/SBS-CMA segregation.

Despite these promising results obtained in the laboratory, further researches are needed before the industrial use of CR/SBS-CMA containing Sasobit. Future researches are required to conduct a comprehensive study on the various properties of CR/SBS-CMA mixtures containing Sasobit and pave test road to test the performance of CR/SBS-CMA pavements.

CRediT authorship contribution statement

Lin Peng: Writing – review & editing. **Li Yang:** Investigation, Writing – review & editing. **Zhao Kangzhi:** Writing – original draft, Methodology, Investigation, Data curation, Conceptualization. **Meng Yuanyuan:** Supervision, Investigation. **He Fuqiong:** Writing – original draft, Supervision, Investigation. **Ye Xiangqian:** Supervision, Investigation. **Hu Chichun:** Supervision, Methodology, Funding acquisition,

Conceptualization.

Declaration of Competing Interest

The authors declare that they have no known competing financial interests or personal relationships that could have appeared to influence the work reported in this paper.

Acknowledgements

This research was supported by the Guangzhou Expressway Management Co. LTD ((2021)-040).

Data availability

Data will be made available on request.

References

- [1] A. Behnood, M.M. Ghareveran, Morphology, rheology, and physical properties of polymer-modified asphalt binders, *Eur. Polym. J.* 112 (2019) 766–791.
- [2] R.S. Mullapudi, Restriction of RAP% in HMA based on aggregate gradation and binder properties, *CivilEng* 2 (2021).
- [3] J. Nithinchary, B.P. Dhandapani, R.S. Mullapudi, Application of warm mix technology - design and performance characteristics: review and way forward, *Constr. Build. Mater.* 414 (2024) 24.

[4] Y. Pei, S.Q. Jiang, Z. Ding, L.D. Cheng, P.L. Li, X.M. Jiang, Preparation and performance analysis of high-viscosity asphalt containing high-content SBS and crumb rubber by oxygen-free high-temperature treatment, *Constr. Build. Mater.* 402 (2023) 13.

[5] J.D. Huang, Q.A. Wang, RETRACTION: Influence of crumb rubber particle sizes on rutting, low temperature cracking, fracture, and bond strength properties of asphalt binder (Retraction of Vol 54, Pg 54, 2021), *Mater. Struct.* 55 (2) (2022) 1.

[6] M.Y. Chen, J.G. Geng, C.Y. Xia, L.L. He, Z. Liu, A review of phase structure of SBS modified asphalt: affecting factors, analytical methods, phase models and improvements, *Constr. Build. Mater.* 294 (2021) 22.

[7] B. Liang, K. Shi, Y.F. Niu, Z.C. Liu, J.L. Zheng, Probing the modification mechanism of and customized processing design for SBS-modified asphalts mediated by potentiometric titration, *Constr. Build. Mater.* 234 (2020) 8.

[8] A. Behnood, A. Shah, R.S. McDaniel, M. Beeson, J. Olek, High-temperature properties of asphalt binders comparison of multiple stress creep recovery and performance grading systems, *Transp. Res. Rec.* 2574 (2016) 131–143.

[9] H.L. Zhang, Z.H. Chen, G.Q. Xu, C.J. Shi, Evaluation of aging behaviors of asphalt binders through different rheological indices, *Fuel* 221 (2018) 78–88.

[10] P. Lin, W.D. Huang, Y. Li, N.P. Tang, F.P. Xiao, Investigation of influence factors on low temperature properties of SBS modified asphalt, *Constr. Build. Mater.* 154 (2017) 609–622.

[11] Y. Gong, J. Xu, R. Chang, E.H. Yan, Effect of water diffusion and thermal coupling condition on SBS modified asphalts' surface micro properties, *Constr. Build. Mater.* 273 (2021) 12.

[12] P. Lin, C.Q. Yan, W.D. Huang, Y. Li, L. Zhou, N.P. Tang, F.P. Xiao, Y. Zhang, Q. Lv, Rheological, chemical and aging characteristics of high content polymer modified asphalt, *Constr. Build. Mater.* 207 (2019) 616–629.

[13] J. Li, F.P. Xiao, S.N. Amirkhanian, High temperature rheological characteristics of plasma-treated crumb rubber modified binders, *Constr. Build. Mater.* 236 (2020) 14.

[14] L.G. Picado-Santos, S.D. Capitao, J.M.C. Neves, Crumb rubber asphalt mixtures: a literature review, *Constr. Build. Mater.* 247 (2020) 13.

[15] D.A. Simon, T. Bárány, Microwave devulcanization of ground tire rubber and its improved utilization in natural rubber compounds, *ACS Sustain. Chem. Eng.* 12 (2023).

[16] Y. Wen, Y.H. Wang, K.C. Zhao, D. Chong, W.D. Huang, G.R. Hao, S.C. Mo, The engineering, economic, and environmental performance of terminal blend rubberized asphalt binders with wax-based warm mix additives, *J. Clean. Prod.* 184 (2018) 985–1001.

[17] S.J. Liu, A.H. Peng, J.T. Wu, S.B. Zhou, Waste engine oil influences on chemical and rheological properties of different asphalt binders, *Constr. Build. Mater.* 191 (2018) 1210–1220.

[18] I.A. Qurashi, A.K. Swamy, Viscoelastic properties of recycled asphalt binder containing waste engine oil, *J. Clean. Prod.* 182 (2018) 992–1000.

[19] W.C. Huang, Y. Li, Y.Y. Meng, C. He, X.Q. Ye, X.R. Chen, C.C. Hu, Comprehensive study on the performance of SBS and crumb rubber composite modified asphalt based on the rubber pretreatment technology, *Case Stud. Constr. Mater.* 20 (2024) 17.

[20] Y.J. Zhang, P. Xiao, P. Qian, X.K. Deng, A.H. Kang, Z.F. Wang, Y.Q. Li, Probe the properties of SBS/CR composite modified asphalt with CR directional distribution, *Constr. Build. Mater.* 411 (2024) 19.

[21] Z.H. Yang, L.B. Wang, X. Bin, D.W. Cao, J.F. Li, K. Zhao, Performance of SBS modifier-crumb rubber composite modified asphalt used as an anti-wear layer of perpetual pavement, *Int. J. Pavement Eng.* 15 (2021).

[22] H. Nan, Y. Sun, J. Chen, M. Gong, Investigation of fatigue performance of asphalt binders containing SBS and CR through TS and LAS tests, *Constr. Build. Mater.* (2022).

[23] Y. Erkut, B.V. Kök, M. Yilmaz, Evaluation of performance and productivity of bitumen modified by three different additives, *Constr. Build. Mater.* 261 (2020) 12.

[24] M. Lagos-Varas, D. Movilla-Quesada, A.C. Raposeiras, P. Monsalve-Carcamo, D. Castro-Fresno, Rheological analyses of binders modified with triple combinations of Crumb-Rubber, Sasobit and Styrene-Butadiene-Styrene, *Case Stud. Constr. Mater.* 19 (2023) 16.

[25] M.O. Hamzah, B. Golchin, A. Jamshidi, E. Chailleux, Evaluation of Rediset for use in warm-mix asphalt: a review of the literatures, *Int. J. Pavement Eng.* 16 (9) (2015) 809–831.

[26] B. Liang, H.T. Zhang, Y. Liang, X.F. Wang, J.L. Zheng, Review on warm mixing asphalt technology, *J. Traffic Transp. Eng.* (2023) 24–46.

[27] J.H. Gao, K.Z. Yan, W.L. He, S.F. Yang, L.Y. You, High temperature performance of asphalt modified with Sasobit and Deurex, *Constr. Build. Mater.* 164 (2018) 783–791.

[28] S.F. Yang, K.Z. Yan, W.L. He, Z.G. Wang, Effects of Sasobit and Deurex additives on asphalt binders at midrange and high temperatures, *Int. J. Pavement Eng.* 20 (12) (2019) 1400–1407.

[29] Z.H. Chen, H.L. Zhang, H.H. Duan, C.J. Shi, Improvement of thermal and optical responses of short-term aged thermochromic asphalt binder by warm-mix asphalt technology, *J. Clean. Prod.* 279 (2021) 13.

[30] A. Jamshidi, M.O. Hamzah, Z.P. You, Performance of warm mix asphalt containing Sasobit®: State-of-the-art, *Constr. Build. Mater.* 38 (2013) 530–553.

[31] M.J. Yue, J.C. Yue, R.R. Wang, Y.C. Xiong, Evaluating the fatigue characteristics and healing potential of asphalt binder modified with Sasobit® and polymers using linear amplitude sweep test, *Constr. Build. Mater.* 289 (2021) 19.

[32] M.J. Yue, J.C. Yue, R.R. Wang, Y.J. Guo, X.P. Ma, A comprehensive analysis of fatigue and healing capacity of sasobit polymer-modified asphalt from two perspectives: binder and FAM, *J. Mater. Civ. Eng.* 35 (3) (2023) 19.

[33] G.C. Hurley, B.D. Prowell, Evaluation of Sasobit® for use in warm-mix asphalt, *ncat report* (2005).

[34] X. Yang, J. Mills-Beale, Z. You, Chemical characterization and oxidative aging of bio-asphalt and its compatibility with petroleum asphalt, *J. Clean. Prod.* 142 (2017) 1837–1847.

[35] J.Y. Wang, J. Yuan, K.W. Kim, F.P. Xiao, Chemical, thermal and rheological characteristics of composite polymerized asphalts, *Fuel* 227 (2018) 289–299.

[36] Y.Y. Meng, X.Q. Ye, F.Q. He, Z.P. Chen, C.C. Hu, P. Lin, Comprehensive study on the degradation progress of crumb tire rubber during the preparation of terminal blended rubberized asphalt binder, *J. Clean. Prod.* 417 (2023) 14.

[37] C. Hintz, R. Velasquez, C. Johnson, H. Bahia, Modification and validation of linear amplitude sweep test for binder fatigue specification, *Transp. Res. Rec.* 2207 (2011) 99–106.

[38] A. Behnood, J. Olek, Rheological properties of asphalt binders modified with styrene-butadiene-styrene (SBS), ground tire rubber (GTR), or polyphosphoric acid (PPA), *Constr. Build. Mater.* 151 (2017) 464–478.

[39] J.X. Zhang, D.W. Yang, G.Q. Sun, Y.W. Li, Y. Qi, X.Y. Ma, Roles of recycled oils, polyphosphoric acid and sulfur on chemo-rheological and morphological properties of high-viscosity modified asphalt, *Constr. Build. Mater.* 371 (2023) 13.

[40] T. Lu, B. Hofko, D.Q. Sun, J. Mirwald, L. Eberhardsteiner, M.J. Hu, Microscopic and rheologic characterization of third generation self-repairing microcapsule modified asphalt, *Constr. Build. Mater.* 400 (2023) 10.

[41] S.D. Capitao, L.G. Picado-Santos, F. Martinho, Pavement engineering materials: Review on the use of warm-mix asphalt, *Constr. Build. Mater.* 36 (2012) 1016–1024.

[42] C.J. Liu, Q.P. Wang, Enhancing effect of waste engine oil bottom incorporation on the performance of CR plus SBS modified bitumen: a sustainable and environmentally-friendly solution for wastes, *Sustainability* 13 (22) (2021) 20.

[43] K.L. Roja, M.F. Aljarrah, N.M. Sirin, Eyad, rheological, thermal, and chemical evaluation of asphalt binders modified using crumb rubber and warm-mix additive, *J. Mater. Civ. Eng.* 34 (5) (2022).

[44] G.J. Zhao, P. Guo, Workability of Sasobit Warm Mixture Asphalt, *International Conference on Future Energy, Environment, and Materials (FEEM) (PEOPLES R CHINA)*, Elsevier Science Bv, Hong Kong, 2012, pp. 1230–1236 (PEOPLES R CHINA).

[45] C.D. Qian, W.Y. Fan, G.M. Yang, L. Han, B.D. Xing, X.B. Lv, Influence of crumb rubber particle size and SBS structure on properties of CR/SBS composite modified asphalt, *Constr. Build. Mater.* 235 (2020) 13.

[46] S.Q. Zhao, Q.L. You, C. Jian, T. Sesay, H.L. Qiao, S.T. Tian, Improving storage stability and rheological performance of asphalt rubber modified with nanosilica and Sasobit, *Road. Mater. Pavement Des.* (2024) 25.

[47] G.D. Airey, Rheological properties of styrene-butadiene styrene polymer modified road bitumens, *Fuel* 82 (14) (2003) 1709–1719.

[48] M. Ameri, D. Mirzaian, A. Amini, Rutting resistance and fatigue behavior of gilsonite-modified asphalt binders, *J. Mater. Civ. Eng.* 30 (11) (2018) 9.

[49] D. Yu, Y.X. Gu, X. Yu, Rheological-microstructural evaluations of the short and long-term aged asphalt binders through relaxation spectra determination, *Fuel* 265 (2020) 8.

[50] A. Subhy, Advanced analytical techniques in fatigue and rutting related characterisations of modified bitumen: literature review, *Constr. Build. Mater.* 156 (2017) 28–45.

[51] Y.R. Sun, W.Y. Wang, J.Y. Chen, Investigating impacts of warm-mix asphalt technologies and high reclaimed asphalt pavement binder content on rutting and fatigue performance of asphalt binder through MSCR and LAS tests, *J. Clean. Prod.* 219 (2019) 879–893.

[52] A. Mansourian, M. Ameri, M.H. Mirabi moghaddam, E. Riahi, H. Shaker, A. H. Ameri, Behavioural mechanism of SBR, LDPE, and SBS modified bituminous mixtures, *Aust. J. Civ. Eng.* (2022) 389–398.

[53] Y. Li, W.C. Huang, S.H. Zhao, Z.X. Yan, F.Q. He, C.C. Hu, S. Shen, Influence of rejuvenator components on rheological properties of recycled bitumen in the full temperature range, *Constr. Build. Mater.* 414 (2024) 15.

[54] Y.Y. Meng, L. Zhan, C.C. Hu, Y.K. Tang, D. Grobeger, X.Q. Ye, Research on modification mechanism and performance of an innovative bio-based polyurethane modified asphalt: a sustainable way to reducing dependence on petroleum asphalt, *Constr. Build. Mater.* 350 (2022) 13.

[55] U.A. Mannan, H.M. Faisal, R.A. Tarefder, Creep stiffness master curve of recycled asphalt pavement (RAP) modified asphalt binders based on binder beam rheometer (BBR) test data, *Int. Conf. Highw. Pavements Airfield Technol. Am. Soc. Civ. Eng.* (2017) 246–255.

[56] Z.J. Dong, T. Zhou, H. Luan, R.C. Williams, P. Wang, Z. Leng, Composite modification mechanism of blended bio-asphalt combining styrene-butadiene-styrene with crumb rubber: a sustainable and environmental-friendly solution for wastes, *J. Clean. Prod.* 214 (2019) 593–605.

[57] M. Akpolat, Investigation of rutting, fatigue and cracking resistance parameters of CR modified warm asphalt binders compare with SBS modified binders, *Rev. Constr. 21 (2) (2022) 309–328.*

[58] P.P. Kong, G. Xu, L.X. Fu, H.X. Feng, X.H. Chen, Chemical structure of rubber powder on the compatibility of rubber powder asphalt, *Constr. Build. Mater.* 392 (2023) 16.